

# The Difficult Chore of Measuring Coordination by EXAFS

B. Ravel and S. D. Kelly

Biosciences Division, Argonne National Laboratory, Argonne, IL 60439, USA

**Abstract.** Neither the theory nor the interpretation of Extended X-Ray-Absorption Fine-Structure (EXAFS) spectroscopy requires assumptions of crystalline symmetry or periodicity. As a result, EXAFS is a tool applied to a wide range of scientific disciplines and to a wide variety of experimental systems. A simple enumeration of the atoms in the coordination environment of the absorber is often the primary goal of an EXAFS experiment. There are, however, a number of pitfalls in the way of an accurate determination of coordination number (CN). These include statistical limitations of the EXAFS fitting problem, empirical effects due to sample preparation, and the assumptions made about the physical structure surrounding the absorber in the course of data analysis. In this paper we examine several of these pitfalls and their effects upon the determination of CN. Where possible, we offer suggestions for avoiding or mitigating the pitfalls. We hope this paper will help guide the general EXAFS practitioner through the difficult chore of accurately determining CN.

**Keywords:** data analysis, coordination number

**PACS:** 78.70.Dm, 61.10.Ht

Extended X-ray-absorption fine-structure (EXAFS) is an ideal probe for measuring coordination chemistry in systems spanning an impressively broad array of scientific disciplines. In many cases, the evaluation of coordination number (CN) is the principle goal of an EXAFS experiment. Although the problem of using EXAFS to determine CN is easily stated, we find that newcomers to EXAFS analysis frequently stumble over a number of common pitfalls. In this paper, we discuss several of these common pitfalls and provide some suggestions to help in the accurate determination of CN.

*Passive Electron Reduction Factor.* The multiple scattering formalism implemented by FEFF [1] and others provides a convenient framework for the analysis of EXAFS spectra. The measured fine structure  $\chi(k)$  is understood as the sum of the contributions from all the ways that the photoelectron can scatter from the neighboring atoms. The contribution for any given scattering geometry can be expressed by Eq. (1) and the contributions for all scattering geometries (denoted  $\Gamma$ ) are summed as in Eq. (2) to yield the total  $\chi(k)$ .

$$\chi_{\Gamma}(k) = \frac{N_{\Gamma} S_0^2 F_{\Gamma}(k)}{2kR_{\Gamma}^2} e^{-2k^2\sigma_{\Gamma}} e^{-2R_{\Gamma}/\lambda(k)} \times \quad (1)$$

$$\sin(2kR_{\Gamma} + \Phi_{\Gamma}(k) - 4k^3 C_{3,\Gamma}/3) \quad (2)$$

$$\chi_{\text{total}} = \sum_{\Gamma} \chi_{\Gamma}(k)$$

The scattering amplitude  $F_{\Gamma}(k)$  and phase shift  $\Phi_{\Gamma}(k)$  are computed by the theory program, as is the photoelectron mean free path  $\lambda(k)$ . The other terms in Eq. (1) are parameterized and determined by non-linear analysis.

CN,  $N_{\Gamma}$  in Eq. (1), represents the number of atoms which are at the same distance from the absorbing atom

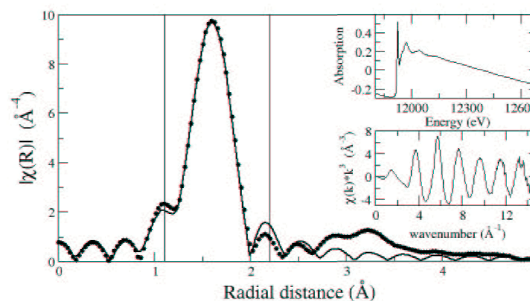


**FIGURE 1.** A simple fit to the first shell in aqueous gold hydroxide. The vertical lines indicate the fitting range. The insets show the raw data and the background-subtracted  $\chi(k)$ .

and which contribute identically to the measured spectrum. Without any further discussion of the mechanics of parameterizing Eq. (1), we see two challenges to determining  $N_{\Gamma}$ .  $N_{\Gamma}$  is multiplied by  $S_0^2$ , the passive electron reduction factor, and by the scattering amplitude  $F_{\Gamma}(k)$ .  $S_0^2$  is a correction to the theory [1] accommodating the relaxation of the outer shell electrons in the presence of core-hole. It is well approximated by a number and is typically between 0.7 and 1.0, but it is not known *a priori* for any element. Because  $N_{\Gamma}$  and  $S_0^2$  are multiplied in Eq. (1), they are, for a single shell fit, indistinguishable in a statistical sense and cannot be independently refined. Since  $S_0^2$  is a parameter of the absorber while  $N_{\Gamma}$  is a parameter of the scatterer, they may be distinguishable in a fit to multiple shells.

Consider a first shell fit. Fig. 1 shows data measured on the gold  $L_{III}$  edge of aqueous gold hydroxide. There, the gold atom is surrounded by the O atoms of a hydration shell. The fitting model used a Gaussian distribution of O

atoms, thus the fitting parameters included an amplitude, a shift to the centroid ( $R$  in Eq. (1)), a width of the distribution ( $\sigma^2$  in Eq. (1)), and a shift to the energy reference,  $E_0$ . The amplitude was refined to  $3.58 \pm 0.40$ .

Any interpretation of the measured amplitude requires confidence in the calculation of  $F_{\Gamma}(k)$  for the Au–O pair, which in this case was made with FEFF6. The theory of absorption spectroscopy, although well-established, is still developing. Any error in the calculation of  $F_{\Gamma}(k)$  becomes a systematic error in the measure of the amplitude.

How many O atoms surround the gold atom? Given the range of expected values for  $S_0^2$ , there may be less than 4 or more than 5. One way to determine the CN is to analyze a known material and to assert *chemical transferability*, i.e. that  $S_0^2$  for two materials measured under similar conditions will be the same. Asserting this and performing a fit to the four shells of gold metal using all relevant single and multiple scattering paths yields  $S_0^2 = 0.89 \pm 0.06$ . Using this and propagating uncertainties yields  $N_{\Gamma} = 4.02 \pm 0.52$  for the aqueous gold hydroxide. Another approach is to use FEFF8 or other theory to compute  $S_0^2$  directly.

**Sample Preparation.** Accurate determination of CN starts before the sample is measured. Good sample preparation is essential to measuring high quality data. Distortions to data due to sample inhomogeneity [2, 3] will distort both the amplitude of  $\chi(k)$  and the measured values for  $\sigma^2$ . Poor sample preparation introduces the same systematic error into the determination of CN as an incorrect calculation of  $F_{\Gamma}(k)$  or determination of  $S_0^2$ .

Measurements made in fluorescence face an additional challenge. The depth to which the incident beam penetrates changes with energy as  $\chi(k)$  oscillates. This effect, known variously as *self-absorption* or *over-absorption*, attenuates both the amplitude and the measured  $\sigma^2$  values. While it is possible to approximately correct [4] for this effect after the fact using knowledge of the measured system, it is prudent to avoid the problem when possible using good sample preparation practices.

**Normalization.** A common approach to data analysis is to isolate  $\chi(k)$  from the  $\mu(E)$  spectrum by removing [5] the background function. The  $\chi(k)$  is typically normalized to have unit edge step. This normalization is found [6] regressing a line to pre-edge region and regressing a quadratic polynomial to the post-edge region. These polynomials are extrapolated back to the edge energy where the difference between them is used as the normalization constant.

Fig. 2 shows the post-edge regression for data from a  $U^{6+}$  species measured in fluorescence. The top shows the post-edge regression using the default parameterization of the ATHENA [7, 6] program. The bottom shows the same data, but with parameters chosen such that the

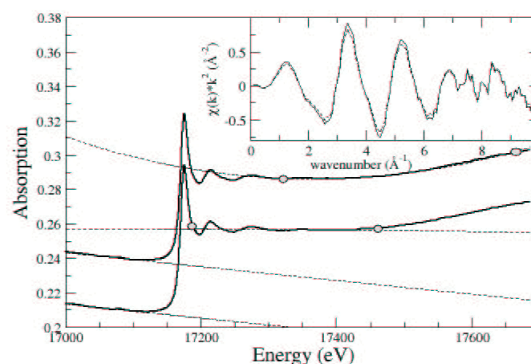


**FIGURE 2.** Effect of normalization parameters on the evaluation of the edge step normalization for a  $U^{6+}$  compound. The circles show the range over which the post-edge regressions were performed. The inset shows the extracted  $\chi(k)$ .

white line was of the same height as a  $U^{6+}$  standard believed to be the same material. The difference in amplitude of  $\chi(k)$  seen in the inset is the result of the difference in the post-edge polynomials and will introduce error into the determination of CN from these data. To avoid this error, one must use a clear criterion for choosing the parameterization of the post-edge polynomial, as was done for the bottom spectrum in Fig. 2.

**Non-Gaussian Distributions: Solutions.** Implicit to the determination of CN for the aqueous gold hydroxide, was the assumption that the hydration shell was Gaussian distributed about the gold atom. It is well-known that the radial distribution of water molecules around solvated metal atoms [8] is a highly skewed function that is poorly approximated by a Gaussian distribution. The value obtained for the CN can only be considered accurate insofar as we believe the function used to describe the distribution of water about the gold.

A common approach to non-Gaussian distributions is the cumulant expansion. [9] This approach, however, becomes increasingly inaccurate [10] as the distribution becomes increasingly disordered. Codes like FEFF which use the path expansion of Eq. (2) can be used to model non-Gaussian distributions by discrete integration over any distribution function. A histogram with bins placed on a grid over the range of the distribution function is used. A path is placed at each bin and the height of the bin is set to the value of the distribution function at that grid point. The distribution function used in Ref.[8] can be successfully reproduced using this approach.

This histogram approach to data analysis is extremely flexible and well-suited for complicated systems. Indeed, it shines for multi-model distributions. The remainder of this paper outlines this approach for complicated material systems.

**Barium Tantalum Oxynitride.** In a recent publication, the local disorder in the nominally cubic oxynitride perovskite BaTaO<sub>2</sub>N was examined. [11] An attempt to fit Ta *K*-edge data using a cumulant model for the near-neighbor atoms was unsuccessful. The quality of the fits was poor, as seen in Figure 3 and the fit parameters refined to confusing, unphysical values.

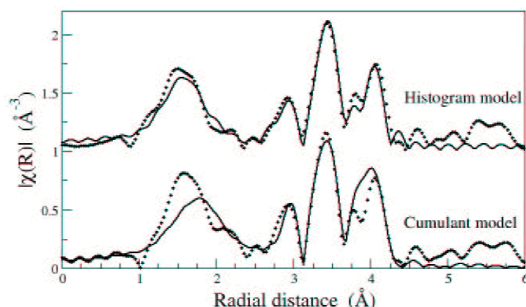


**FIGURE 3.** Fits to the BaTaO<sub>2</sub>N Ta *K*-edge data measured at 100 K data using the cumulant and histogram models.

The fitting model was recast using the results of a total energy minimization as the basis of the structural model. This theory introduced significant local distortion due to the differing ionic radii and electronegativities of the O and N atoms, with O drawn closer to the Ta absorber and N pushed away. This results in a multi-model distribution of atoms in the first and third coordination shells.

All atom pairs from the energy minimization which involved Ta were extracted from the box and pairs with similar distances were gathered into histogram bins 0.02 Å wide. A FEFF calculation was used for the contribution from each bin, as in Eq. (1), with the population of the bin replacing the  $N_T$  term. This model, shown at the top of Figure 3, is not only an improvement to the fit, but yielded physically reasonable parameters.

**Hydrated Zinc on Titanium Oxide.** In a recent publication [12] the placement of Zn ions adsorbed onto rutile was examined by EXAFS, x-ray standing waves (XWS), and density functional theory (DFT). Aqueous Zn is typically coordinated by 6 O atoms, but may be coordinated by only 4 O in a crystal. Zn adsorbed onto the rutile surface is expected to be 4 or 6 fold coordinated. Polarized dependent EXAFS data was collected at the Zn *K*-edge and co-refined to determine CN.

Modeling the data with a Gaussian distribution of O yielded seemingly good fits, but with CN ranging from 5 to 13 and with very large  $\sigma^2$  values of  $\sim 0.020^2$ . A value of  $\sim 0.002^2$  is typical for a Zn–O bond.

The DFT calculations found several possible sites for Zn on the Rutile surface. Using the theory-derived structures shown in Figure 4 along with a fraction of aqueous Zn, the data at all three polarization were fit well,

including higher shells, with physically sensible parameters and in agreement with the XSW measurements. The O distribution about Zn on the rutile surface is poorly described by a Gaussian.

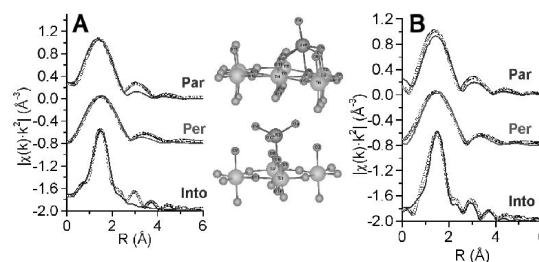


**FIGURE 4.** Fits to polarization dependent data of Zn adsorbed onto rutile using a Gaussian distribution (A) and the DFT-derived structure (B).

Accurate determination of CN is not trivial in EXAFS data analysis. At best, CN must be interpreted from the amplitude term refined in a fit. For complicated systems, accurate determination of CN requires sophisticated structural modeling. References [13] and [14] offer two more examples of using a path expansion for complicated distributions. A variety of useful tutorials and presentations discussing the many issues covered in this short paper can be found on the web at XAFS.ORG. [15]

## REFERENCES

1. J. J. Rehr, and R. C. Albers, *Rev. Mod. Phys.* **73**, 621–654 (2000).
2. K. Q. Lu, and E. A. Stern, *Nuc. Inst. Meth.* **212**, 475–478 (1983).
3. E. A. Stern, and K. Kim, *Phys. Rev. B* **23**, 3781–3787 (1981).
4. C. Booth, and F. Bridges, *Physica Scripta* **T115**, 202–204 (2005).
5. M. Newville, P. Līviņš, Y. Yacoby, J. J. Rehr, and E. A. Stern, *Phys. Rev. B* **47**, 14126–14131 (1993).
6. B. Ravel, and M. Newville, *J. Synchrotron Radiat.* **12**, 537–541 (2005).
7. M. Newville, *J. Synchrotron Radiat.* **8**, 322–324 (2001).
8. P. D'Angelo, V. Barone, G. Chillemi, N. Sanna, W. Meyer-Klaucke, and N. Pavel, *J. Am. Chem. Soc.* **124**, 1958–1967 (2002).
9. G. Bunker, *Nuc. Inst. Meth.* **207**, 437–444 (1983).
10. A. Filipponi, *J. Phys.: Condens. Matter* **13**, R23–R60 (2001).
11. B. Ravel, Y.-I. Kim, P. Woodward, and C. Fang, *Phys. Rev. B* **73**, 184121 (2006).
12. Z. Zhang, P. Fenter, S. Kelly, J. Catalano, A. Bandura, J. Kubicki, J. Sofo, D. Wesolowski, M. Machesky, N. Sturchio, and M. Bedzyk, *Geochim. Cosmochim. Acta* (2006), accepted.
13. S. Webb, B. Tebo, and J. Bargar, *Am. Mineralogist* **90**, 1342–1357 (2005).
14. B. Ravel, E. Cockayne, M. Newville, and K. M. Rabe, *Phys. Rev. B* **60**, 14632–146462 (1999).
15. XAFS.ORG, a community web site for XAFS and related techniques, <http://xafs.org> (2006).